Optics Communications 290 (2013) 132–135

Contents lists available at SciVerse ScienceDirect

Optics Communications

journal homepage: www.elsevier.com/locate/optcom

Low-threshold and compact multicolored femtosecond laser generated by using cascaded four-wave mixing in a diamond plate

Jinping He [a,b], Juan Du [a,b], Takayoshi Kobayashi [a,b,c,d,*]

[a] Advanced Ultrafast Laser Research Center, University of Electro-Communications, 1-5-1 Chofugaoka, Chofu, Tokyo 182-8585, Japan
[b] JST, CREST, 5 Sanbancho, Chiyoda-ku, Tokyo 102-0075, Japan
[c] Department of Electrophysics, National Chiao-Tung University, 1001 Ta Hsinchu Rd., Hsinchu 300, Taiwan
[d] Insitute of Laser Engineering, Osaka University, 2-6 Yamada-oka, Suita, Osaka 565-0971, Japan

ARTICLE INFO

Article history:
Received 10 August 2012
Received in revised form
12 October 2012
Accepted 17 October 2012
Available online 1 November 2012

Keywords:
Multicolor laser
Cascaded four-wave mixing
2-D multicolor arrays
Beam breakup

ABSTRACT

Low-threshold and compact multicolored laser generated by cascaded four-wave mixing in a diamond plate is demonstrated. The spectra and output energy of the generated sidebands up to 2nd order on the Stokes side and >12th on the anti-Stokes side covering from near infrared to UV, are shown. The 2-D multicolor arrays were also observed in diamond plate with low threshold and explained briefly. The compact wavelength-tunable multicolored laser setup is promising to be used in spectroscopy experiments, for example multicolor pump-probe experiments.

1. Introduction

Recently, cascaded four-wave mixing (CWFM) processes have been shown to be effective in generation of wavelength-tunable multicolored femtosecond pulses, which are useful in applications including spectroscopy experiments, such as multicolored pump-probe experiments [1], femtosecond CARS spectroscopy [2], and two-dimensional spectroscopy [3]. The extension of spectral width of the generated pulses is covering a range broader than 1.5 octaves, and the spectra were continuously tunable [4]. The pulse duration shorter than 40 fs and RMS power stability less than 1% make them very attractive [5]. However, two beams are needed to be prepared for CWFM, such as a hollow fiber [6,7], a dye-laser-amplifier system [8], and an optical parameter amplifier [9], which requires expensive and complicated experimental setup. A new fiber-based laser source, femtosecond Cherenkov radiation [10,11] with compact experimental setup, tunable wavelength, and low-threshold, has the potential to be used to generate multicolor laser if the central wavelength difference of the two beams could be smaller. It is practically valuable to construct a more compact and inexpensive multicolored laser system.

Except for the one-dimensional multicolored array mentioned above, two-dimensional (2-D) multicolored transverse arrays were also generated in quadratic nonlinear medium [12] and third-order nonlinear media [4] under the pump of two noncollinear cross-overlapped femtosecond beams. The 2-D multicolor array generated in quadratic nonlinear medium was attributed to multiple quadratic spatial solitons generated as a consequence of spontaneous beam breakup due to input asymmetries or material anisotropies [13–16]. Up to now, there is no clear explanation about the 2-D multicolor arrays generated in the process of CWFM, and further experiments and theoretical investigations are needed to understand this new interesting phenomenon.

In this paper, we used only a bulk glass plate to expand the spectrum of a commercial laser, and could get two beams needed for CFWM by filters from the spectrally broadened pulse, which made the experimental setup much more compact and less expensive. The threshold for multicolored laser generation was much lower than silicate glass due to the large nonlinear refractive index of the diamond plate. The bright 2-D multicolored arrays were also observed in this third order nonlinear media with two pump beams for the first time to our knowledge. The threshold energy for the 2-D multicolored arrays generation in a diamond plate is much lower than that in a sapphire plate (0.855 μJ and 0.856 μJ for the diamond plate, 55 μJ and 220 μJ for a sapphire plate) [4].

2. Experimental setup

The experimental setup is shown in Fig. 1. Output pulses with repetition rate/pulse duration/pulse energy of 1 kHz/35 fs/5 mJ from a Ti: sapphire regenerative amplifier laser system (Spitfire

* Corresponding author at: Advanced Ultrafast Laser Research Center, University of Electro-Communications, 1-5-1 Chofugaoka, Chofu, Tokyo 182-8585, Japan. Tel.: +81 42 443 5845; fax: +81 42 443 5826.
E-mail address: kobayashi@ils.uec.ac.jp (T. Kobayashi).

0030-4018/$ - see front matter © 2012 Elsevier B.V. All rights reserved.
http://dx.doi.org/10.1016/j.optcom.2012.10.025

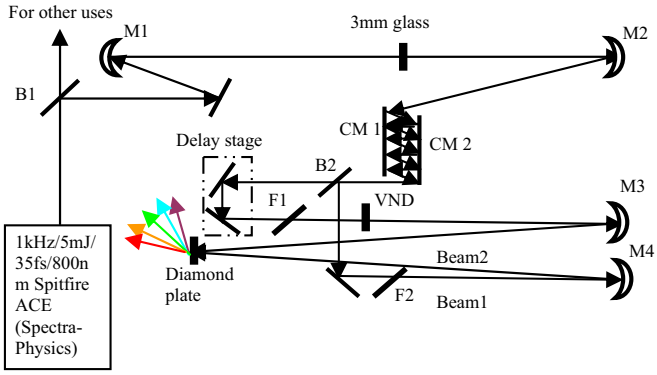

Fig. 1. Experimental setup. B1, B2: beamsplitters; M1–M4: concave mirrors, focal length of M1, M3, and M4 is 500 mm, of M2 is 250 mm; CM1, CM2: chirp mirrors; F1: longpass filter with a cut-off wavelength of 800 nm; F2: shortpass filter with a cut-off wavelength of 800 nm; VND: variable neutral-density filter.

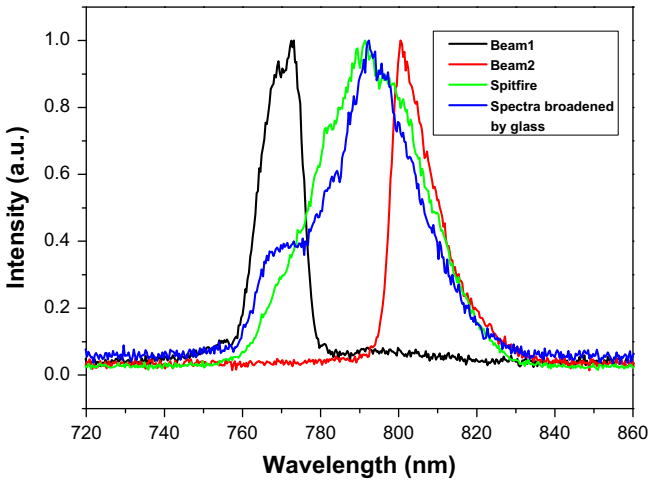

Fig. 2. The spectra of B1 (black), B2 (red), pump laser (Spitfire ACE) (green) and pump laser spectra-broadened by glass (blue). (For interpretation of the references to color in this figure legend, the reader is referred to the web version of this article.)

ACE, Spectra-Physics) was used as the pump source. The pulse after regenerative amplifier was split into two beams by using a beamsplitter. Only ~150 μJ pulse energy was used in the experiment. Then the laser pulse was spectrally broadened by a 3-mm BK7 glass plate, which was placed 20 mm before the focus of M1. After being compressed by a pair of chirp mirrors (CM1, CM2), the laser pulse was split into two beams-Beam1 (B1) and Beam2 (B2). After transmitting through a short pass filter F1 with cut-off wavelength of 800 nm (FES800, Thorlabs), B1 was focused into the nonlinear media by M4. At first B2 passed through a longpass filter F2 with cut-off wavelength of 800 nm (FEL800, Thorlabs) and a variable neutral density (VND) filter and then it was focused into the 1-mm thick diamond plate by M3. The beam diameter was ~300 μm ($1/e^2$ intensity of the peak value) for both B1 and B2 on the diamond plate, and the crossing angle between the two input beams was about 2.2° in air. The size of the present experimental setup is about a half of those used in Refs. [4–7] because of the absence of a hollow fiber and a chamber.

3. Experimental results and discussion

The pulse spectra broadened by glass, B1, and B2 measured by using a commercial spectrometer (USB4000, Ocean Optics) are shown in Fig. 2 together with the femtosecond laser spectrum. There is no supercontinuum generated in the glass plate, and the spectral broadening is due to SPM. The spectrum of B1 (B2) can be adjusted by tuning the angle between input beam and the shortpass filter (longpass filter). The pulse characterization was made by using a home-made FROG and commercial software (FROG 3.0, Femtosoft Technologies). The retrieved temporal intensity profile and the phase are shown in Fig. 3. The durations of the pulse after chirp mirrors, B1, and B2 were measured to be about 26 fs, 81 fs, and 47 fs, respectively.

The pulse energy of B1 was set at 0.855 μJ, and the energy of B2 was continuously adjusted between the VND. The multicolor arrays of different pump powers are shown in Fig. 4. The photographs show the sidebands on a sheet of white paper. The first and second spots from the left edge are B2 and B1, and others are the up-shifted anti-Stokes sidebands (ASi, i=1, 2…). The down-shifted Stokes sidebands (Si, i=1, 2…) are near-infrared pulses, which cannot be detected on the white paper by naked eyes and by the camera as displayed in Fig. 4. In Fig. 4(a), the intensities of B1 and B2 on the diamond plate were 14.9×10^9 W/cm^2 and 12.3×10^9 W/cm^2 respectively, and the thresholds for four-wave mixing in diamond are much lower than fused silica in which two beams of intensities of 60×10^9 W/cm^2 and 8×10^9 W/cm^{2}are needed [17]. 2-D multicolored arrays appeared when the pulse energy of B2 increased to 0.856 μJ as shown in Fig. 4(b). The threshold energy is much lower than that for a sapphire plate (55 μJ and 220 μJ) [4]. When the pulse energy of B2 was increased, the 2-D structure with more anti-Stokes sidebands, more rows and brighter arrays were observed as shown in Fig. 4(c) and (d). No supercontinuum generation or photo-induced damage has been detected even at this enhanced intensity. These stable multicolored arrays are similar to Fig. 2(b) in Ref. [10].The beam breakup due to spatial asymmetric distribution of the input pulse and/or anisotropies in the material was already reported [13,15,18,19]. The cascaded nonlinear processes together with the beam breakup would lead to this new multicolored pattern. The beam breakup is dependent on input energy and beam ellipticity (e) (Fig. 1 in Ref. [13]).When the beam has elliptical cross section with a higher e, the beam breaks up into two. Interestingly, beam breakup was observed even with the near circular (e=1.09) input beam when the input power was ~20 times larger than P_{cr} defined as follows [13]:

$$P_{cr} = 3.77\lambda^2/(8\pi n n_2) \quad (1)$$

where λ is the laser wavelength in vacuum, n the refractive index of the medium at this wavelength, n_2 is the nonlinear refractive index at the relevant wavelength. The spontaneous breakup of elliptical laser beams was also numerically simulated in details by Majus and his coworkers [18]. They attribute this breakup to multistep four-wave and parametric amplification of certain components occurring in the spatial spectrum of the self-focusing laser beam. Because of the asymmetric focusing with several concave reflective mirrors, the input beams exhibited an ellipticity of ~1.2 in our experiment. The peak power of input beams was about ~10^4 times larger than P_{cr} and it was large enough to cause beam breakup [19]. This beam breakup together with CFWM is considered to be the cause of 2-D multicolor structure, as is shown in Fig. 4(b)–(d). It is known that quadratic soliton formation is achieved by coupling of multi-frequency waves in a second-order nonlinear medium. In the process self-trapping occurs as a result of rapid exchange of energy among the multi-frequency waves, which keeps the power and spatial width of the beams mutually stabilized [20]. There is an energy exchange process among the input beams in FWM process [21]. It is very interesting and important if the CFWM process can also lead to multiple spatial solitons. More detailed experimental results and careful theoretic analysis and discussions are needed and in the progress.

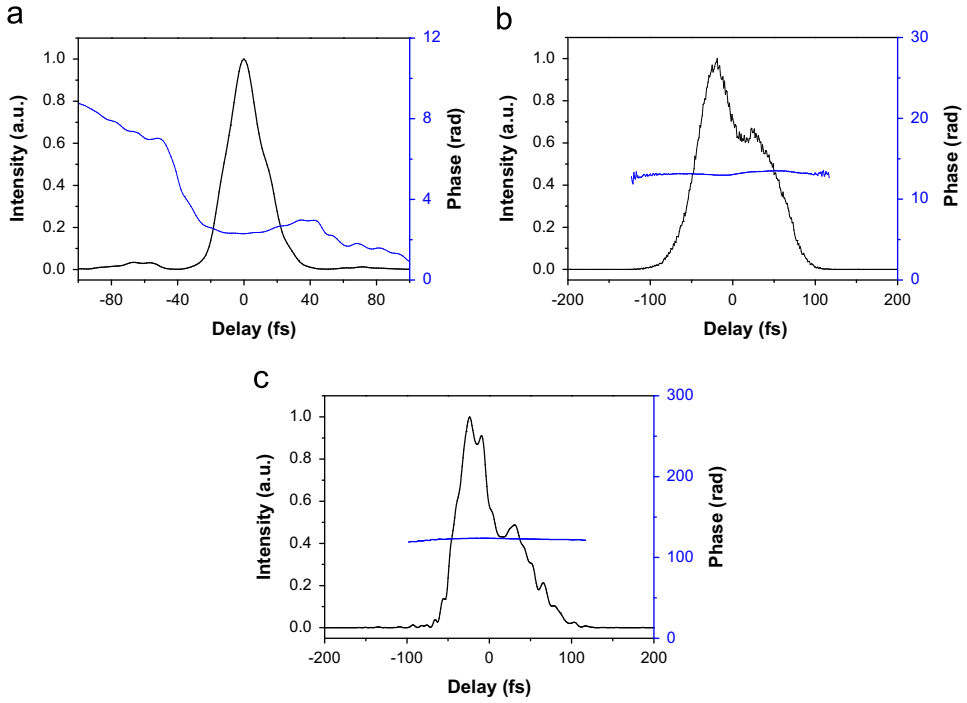

Fig. 3. The FROG retrieved trace of the temporal profile and phase of (a) the pulse spectrum broadened by glass and dispersion compensated by chirp mirrors; (b) B1; (c) B2.

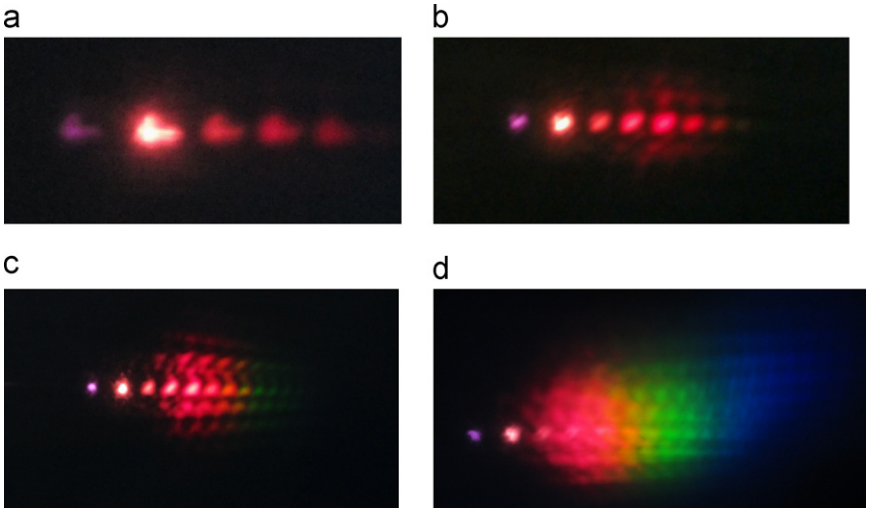

Fig. 4. Patterns of multicolored arrays at different average pump power displayed on a white sheet to paper 10 cm apart from the nonlinear material. (a) B1: 0.855 mW, B2: 0.410 mW; (b) B1: 0.855 mW, B2: 0.856 mW; (c) B1: 0.855 mW, B2: 1.121 mW and (d) B1: 0.855 mW, B2: 1.970 mW.

The normalized spectra of the first five anti-Stokes, two Stokes sidebands, and incident B1 and B2 beams measured using USB4000 are shown in Fig. 5. The spectral width of all the sidebands were broader than 10 nm, which suggest that a pulse duration of < 100 fs can be supported by them. The spectra of all the sidebands can be continuously tuned by changing the crossing angle between B1 and B2, although there is a limit for the tuning range because of the phase-matching condition for CFWM.

Table 1 shows the output power of different sidebands when the pulse energies of B1 and B2 are 0.855 μJ and 0.856 μJ respectively. The conversion efficiency from pump energy to sideband energy was about 1.84%, 1.99%, 0.36%, 0.15%, 0.08%and 0.05% for S1, AS1, AS2, AS3, AS4 and AS5 respectively. The pulse energy is high enough to be used in spectroscopy experiments [1–3]. The power stability of S1 and AS1 was almost the same as the pump beams without any beam point stabilizer which is necessary when a hollow fiber with a small diameter is used in the experiment.

4. Conclusion

In conclusion, low-threshold and compact generation scheme of multicolored pulses by using CFWM in a diamond plate is demonstrated. The properties of the multicolor arrays, spectrum and output energy are shown. The 2-D multicolored arrays were

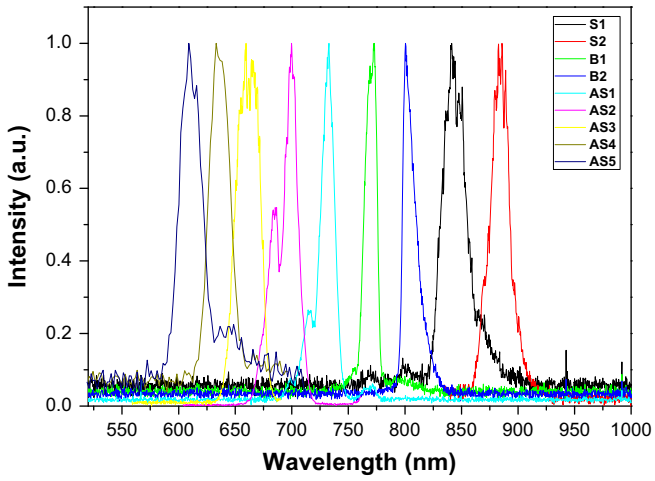

Fig. 5. The normalized spectra of sidebands S1, S2, AS1–AS5, and pump beams B1 and B2.

Table 1
Output power of several sidebands at pump of 0.855 mW and 0.856 mW for B1 and B2, respectively.

	AS1	AS2	AS3	AS4	AS5	S1
Power (μW)	34.0	6.1	2.5	1.3	0.8	31.4

also observed in a diamond plate with lowest threshold among other materials for the first time as far as we know. This setup will be used as a light source for multicolor pump-probe experiments.

Acknowledgment

The authors thank Drs. Jun Liu and Yongliang Jiang for their valuable discussions and technical assistance in the experiments. A part of this work was performed under the joint research project of the Institute of Laser Engineering, Osaka University under Contract no. A3-01.

References

[1] R. Zgadzaj, E. Gaul, N.H. Matlis, G. Shvets, M.C. Downer, Journal of the Optical Society of America B 21 (2004) 1559.
[2] D. Pestov, R.K. Murawski, G.O. Ariunbold, X. Wang, M.C. Zhi, A.V. Sokolov, V.A. Sautenkov, Y.V. Rostovtsev, A. Dogariu, Y. Huang, M.O. Scully, Science 316 (2007) 265.
[3] R.M. Hochstrasser, Proceedings of the National Academy of Sciences 104 (2007) 14190.
[4] J. Liu, T. Kobayashi, Optics Express 16 (2008) 22119.
[5] J. Liu, T. Kobayashi, Z. Wang, Optics Express 17 (2009) 9226.
[6] J. Liu, T. Kobayashi, Optics Express 17 (2009) 4984.
[7] J. Liu, T. Kobayashi, Optics Letters 34 (2009) 2402.
[8] H. Crespo, J.T. Mendonca, A. Dos Santos, Optics Letters 25 (2000) 829.
[9] M. Zhi, X. Wang, A.V. Sokolov, Optics Express 16 (2008) 12139.
[10] H. Tu, S.A. Boppart, Optics Express 12 (2009) 9858.
[11] X. Liu, J. Lægsgaard, U. MΦller, H. Tu, S.A. Boppart, D. Turchinovich, Optics Letters 37 (2012) 2769.
[12] H. Zeng, J. Wu, H. Xu, K. Wu, Physical Review Letters 96 (2006) 083902.
[13] A. Dubietis, G. Tamosauskas, G. Fibich, B. Ilan, Optics Letters 29 (2004) 1126.
[14] S. Polyakov, H. Kim, L. Jankovic, G. Stegeman, Optics Letters 28 (2002) 1451.
[15] Sergey Silvia Carrasco, Hongki Polyakov, Ladislav Kim, Jankovic, George I. Stegeman, Physical Review E 104 (2003) 046616.
[16] R.A. Fuerst, D.M. Baboiu, B. Lawrence, W.E. Torruellas, G.I. Stegeman, Physical Review Letters 78 (2006) 2756.
[17] H. Zhang, H. Liu, J. Si, W. Yi, F. Chen, X. Hou, Optics Express 19 (2011) 12039.
[18] D. Majus, V. Jukna, G. Valiulis, A. Dubietis, Physical Review A 79 (2009) 033843.
[19] N.C. Kothari, T. Kobayashi, Physical Review Letters 50 (1983) 160.
[20] G.I. Stegeman, M. Segev, Science 286 (1999) 1518.
[21] J. Liu, Y. Kida, T. Teramoto, T. Kobayashi, Optics Express 18 (2010) 2495.